INVESTIGATION OF MECHANICAL PROPERTIES OF LUNAR SURFACE MATERIAL AND ITS ANALOGS IN DIFFERENT ATMOSPHERIC CONDITIONS AND IN VACUUM ON THE TOR-1 UNIT

/571

A. I. Vedenin, Ye. A. Dukhovskoy, V. V. Markachev, A. A. Silin, I. I. Cherkasov, and V. V. Shvarev

Abstract

A description is given of the design of measuring assemblies in the TOR-1 instrument along with methods for determining the specific resistance to penetration, compressibility, and the resistance to rotational shearing of lunar surface material and its analogs. Investigations were conducted in helium at normal pressure, as well as in vacuum $5 \cdot 10^{-6}$ torr in the temperature range + (20-140)° C. Values of the specific resistance to penetration of the lunar surface material, coefficients of relative compressibility, and the parameters of the resistance to rotational shearing were obtained for three kinds of compaction of the lunar surface material.

Characteristics of materials investigated. Lunar surface material from the Sea of Fertility returned by the Luna 16 automatic lunar station, and two terrestrial analogs of lunar surface materials were investigated. The first of these is andesite-basaltic volcanic sand from the settlement of Klyuch (Central Kamchatka), and the second is crushed basalt from the Berestovetskiy deposit in the Ukrainian SSR. The data on the chemical, mineralogic, and granulometric composition of all three materials are in Tables 1 and 2.

Under the classification of surface materials SNIP-PB-162 adopted in the USSR, both analogs are categorized as silty sands.

The mineralogic composition of the materials investigated was as follows: the lunar surface material, based on the data of A. P. Vinogradov /1/ contains as the principal minerals plagio-

clases, ilmenite, pyroxene, and olivine, as well as feldspathic rocks (anorthosite). Among the fine grains are encountered monomineralic grains, in which plagioclase, olivine, pyroxene, and ilmenite were identified, as well as spherules and minute dumbbell-shaped objects of volcanic glass. The andesite-basaltic volcanic sand contains disseminations and microlites of plagioclase, pyroxene, hornblende, and ore mineral. The crushed basalt consists of plagioclase, pyroxene, and ore minerals -- magnetite and ilmenite.

The specific weight of the mineral grains of the lunar surface material was assumed to be γ_y = 3.2 g/cm^3; the mean specific weight averaged over the depth of immersion of the Luna 16 drill γ = 1.2 g/cm^3. The specific weight of the mineral grains of the andesite-basaltic volcanic sand γ_y = 2.79 g/cm^3; the specific weight of the grains of crushed basalt γ_y = 2.98 g/cm^3. The specific weight of all three materials varies over wide limits as a function of compaction.

The specific weight in helium was determined by using a graduated beaker 11.3 mm in diameter, into which 1.9 g of the test surface material was poured. The volume it occupied was determined in the friable, heaped state, after compaction by rapping the beaker 50 times against a hard surface, and after additional compaction of the surface material with a plexiglas rod 8 mm in diameter, manually. The experimental results are in Table 3.

Mechanical characteristics of materials subjected to determination. The overall integrated characteristic of strength was taken as the specific resistance to penetration R (kg/cm^2); the angle of internal friction ϕ and the cohesion c (kg/cm^2) were taken as the parameters of resistance to shearing; the coefficient of relative compressibility a_o (cm^2/kg) was taken as the parameter characterizing deformability upon compression. The schemes of the experiments are shown in Fig. 1.

The specific resistance to penetration was determined by the depth of introduction into the surface material of a metal cone with a tip angle α = 30° when a given load P (kg) was applied to it. It was calculated by the formula:

$$R = k\frac{P}{\pi h^2 \operatorname{tg}^2 \frac{\alpha}{2}} \text{ kg/cm}^2 \qquad (1)$$

when $\alpha = 30^{\circ}$:

$$R = 4{,}44\, k_d^{\text{п}} \frac{P}{h^2} \text{ kg/cm}^2. \quad (2)$$

From the penetration results, strength can be computed at the same time, after P. A. Rebinder: /572

$$\tau_R = \frac{P}{h} \cdot \frac{\cos\frac{\alpha}{2}}{\pi \operatorname{tg}\frac{\alpha}{2}} k_d^{\text{п}} \text{ kg/cm}^2; \quad (3)$$

when $\alpha = 30^{\circ}$:

$$\tau_R = 1{,}08 \frac{P}{h^2} k_d^{\text{п}} \text{ kg/cm}^2. \quad (4)$$

A constant relationship exists between the specific resistance to penetration and strength, after P. A. Rebinder, and when $\alpha = 30^{\circ}$, this relationship is:

$$\tau_R \simeq 0{,}25R \text{ kg/cm}^2. \quad (5)$$

The angle of internal friction ϕ and the cohesion c (kg/cm^2) are determined from the Coulomb equation:

$$\tau_{\text{limit}} = \sigma \operatorname{tg}\varphi + c \text{ kg/cm}^2. \quad (6)$$

To calculate ϕ and c, we must conduct no less than two independent determinations of the limiting resistance to shearing τ_{limit} (kg/cm^2) for different values of the normal pressure σ (kg/cm^2).

In our experiments, the limiting resistance to shearing was determined on the rotational shearing instrument with a continuous rotational ribbed disk. During the course of the experiment, the limiting torque causing shearing along the horizontal plane beneath the ribbed disk was determined, and from the value of this moment the limiting resistance to shearing was calculated by the formula:

$$\tau_{\text{limit}} = 2 \frac{M_{\text{limit}}}{\pi r^3} \text{ kg/cm}^2. \quad (7)$$

The angle of internal friction and cohesion were determined by analytical plotting using a rectified plot of the limiting resistance to shearing as a function of the normal pressure on the sample:

$$\varphi = \operatorname{arctg}\left(\frac{\tau - c}{\sigma}\right). \quad (8)$$

TABLE 1. CHEMICAL COMPOSITION*

Material	Chemical constituents and their content, weight percent										
	SiO_2	TiO_2	Al_2O_3	Fe_2O_3	MgO	CaO	Na_2O	K_2O	MnO	Cr_2O_3	ZrO_2
Lunar surface material	41,70	3,39	15,32	16,80[2*]	8,70	12,20	0,37	0,10	0,21	0,31	0,015
Andesite-basaltic volcanic sand	60,35	1,01	15,91	5,56	3,67	5,40	—	—	0,10	—	—
Crushed basalt	49,50	—	17,00	14,50	6,50	9,40	—	—	0,70	—	—

*Composition of lunar surface material is presented based on data of A. P. Vinogradov [1]; the compositions of the other materials are based on the data of the MIIT.++

2* The entire iron content is expressed in terms of FeO.

TABLE 2. GRANULOMETRIC COMPOSITION*

Material	Fraction size, mm							
Andesite-basaltic volcanic sand	7–5 (1,72)	5–3 (3,68)	3–2 (2,56)	2–1 (3,51)	1–0,5 (5,99)	0,5–0,25(10,87)	0,25–0,10 (14,61)	0,10 (57,56)
Crushed basalt	10–5 (0,1)	—	5–2 (0,1)	2–1 (0,5)	1–0,5 (0,6)	0,5–0,25 (2,6)	0,25–0,10 (14,3)	0,10 (81,2)

*Data on the granulometric composition of the lunar surface material are presented in this collection in the paper [2].

Remark. The content (in percentage) is given in parentheses.

The coefficient of relative compressibility a_o (cm^2/kg) during the experiment were continually varied, so that the surface material under the effect of the normal pressure became compacted and its compressibility was reduced. Therefore the coefficient of relative compressibility was calculated separately for the different intervals of normal pressure by the formula:

++ MIIT [Moscow Institute of Railroad Transportation Engineers]

$$a_0 = k_d^{\text{п}} \frac{\Delta s_i}{H_i \Delta p_i} \text{ cm}^2/\text{kg}. \quad (9)$$

The following notation is adopted in the formulas presented above:

- α is the angle at the tip of the penetrometer cone;
- h is the depth of cone penetration into the surface material (cm);
- p is the load on the penetrometer cone (kg);
- M_{limit} is the limiting torque in rotational shearing (kg·cm);
- τ_{limit} is the limiting resistance to shearing (kg/cm^2);
- r is the radius of the ribbed disk (cm);
- σ_i is the normal pressure on the sample (kg/cm^2);
- Δp_i is the increment in the normal pressure over the experimental interval (kg/cm^2);
- H_i is the height of the sample at the beginning of the experimental interval (cm);
- ΔS_i is the reduction in the height of the sample over the experimental interval (cm); and
- $k_d^{\text{п}}$; $k_d^{\text{к}}$ are the coefficients allowing for the effect of the lateral walls on the cylinder on the penetration and compression values.

Use of the scheme of rotational shearing was adopted owing to the small amount of the lunar surface material allocated for the experiments in the TOR-1, with which it was not possible to use ordinary instruments of monoplane shearing or three-axis compression; Eq. (7) was adopted from the data of A. N. Zelenin et al. [3] and presupposes that the plot of the distribution of tangential stresses over the radius of the ribbed disk on attainment of the limiting resistance to shearing is triangular in shape.

Experimental conditions. The experiments were conducted in a TOR-1 vacuum chamber, described in [4]. The vacuum chamber makes it possible to conduct tests in an air atmosphere at normal pressure, in an atmosphere of sterilized, high-purity helium, and in a vacuum up to 10^{-5} torr. The sample temperature can be set at + 20° C (without heating) and up to + 140° C (with heating).

When the experiments were conducted in normal atmospheric conditions, the chamber was not hermeticized and was not evacuated. When the experiments were conducted in a helium atmosphere, preliminary evacuation of the chamber was conducted to a vacuum of $5 \cdot 10^{-5}$ torr, and then it was filled with helium. When the experi-

TABLE 3. SPECIFIC WEIGHT OF LUNAR SURFACE MATERIAL AND ITS ANALOGS

Condition of test material	Specific weight in different states, g/cm^3		
	lunar surface material	andesite-basaltic volcanic sand	crushed basalt
Friable, heaped	1.26	1.05	1.00
Compacted by rapping 50 times	1.90	1.41	1.58
Additionally compacted with a rod	1.90	1.46	1.73

ments were conducted in the vacuum, the chamber was evacuated to $(2-5)\cdot10^{-5}$ torr. In the experiments with heating, the sample was heated before the beginning of the evacuation to evaporate the moisture.

The lunar surface material was placed in a hermetic chamber where it was situated in the atmosphere of pure helium. The analogs of the lunar surface material was sent for testing in exposed form. Because of this, hygroscopic moisture in the amount of 1.5-3.0 percent by weight was present in the analogs. Upon evacuation of the TOR-1, this moisture was evaporated, and subsequent tests in the helium atmosphere and in vacuum were conducted with the dry material. Experience in working with the TOR-1 showed that in the presence of surface materials the evacuation must be conducted slowly, since a rapid pressure drop in the chamber leads to swelling of the surface materials under the effect of the expansion of air in the pores and vaporization through the evaporation of the hygroscopic moisture.

To test the samples, the TOR-1 was equipped with special measuring assemblies mounted on a common panel (see Figs. 2-5). The initial designs of the assemblies, developed in 1970 and described in /4/, were improved based on operating experience so that their operating reliability and precision of measurements were increased. Below are given the descriptions of the improved assemblies.

The sample of the surface material was placed in the central part of the plate within a cylindrical bowl 11.3 mm in diameter. The bowl was equipped with an electric heater. When the experiments were conducted for penetration and compression, the small bowl was immobile. When the experiments were conducted on rotational shearing, it was rotated about a vertical axis.

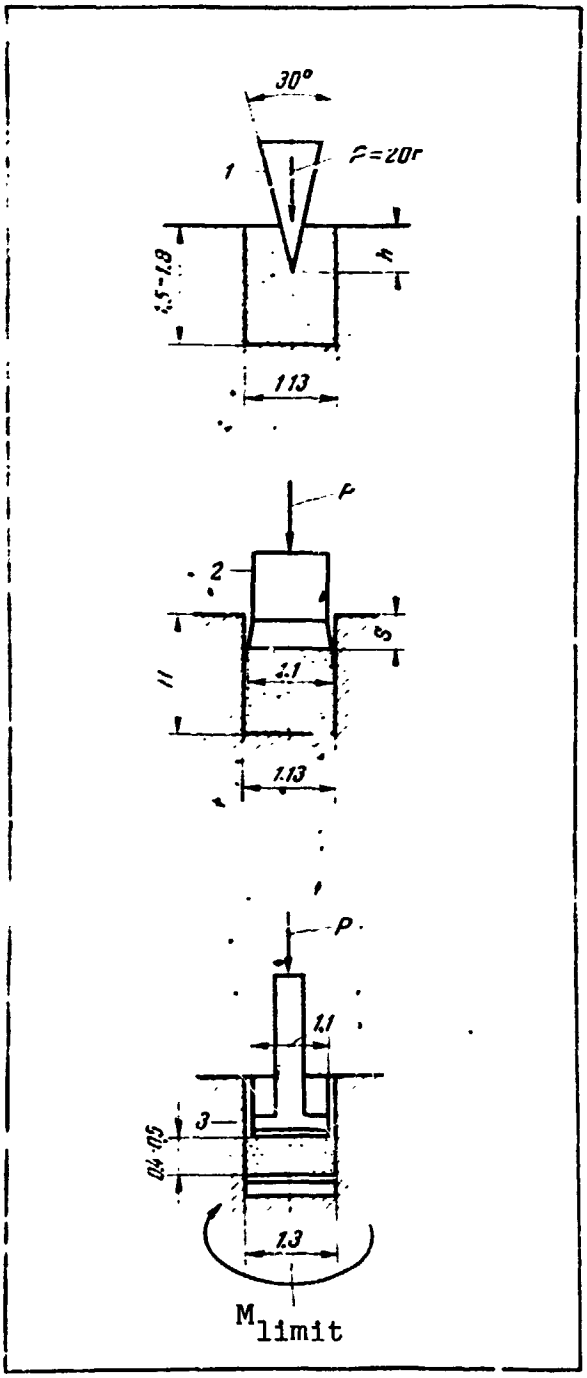

Fig. 1. Schemes for conducting experiments to determine the mechanical parameters of surface material. Above -- penetration; in the middle -- compression; below -- rotational shearing. 1. Cone; 2. Piston; 3. Ribbed disk

The individual measuring assemblies with working parts and devices for applying load and for measuring load and deformation were mounted on cantilevered beams that could be rotated in the vertical plane, bringing the working parts up against the surface of the surface material under study. The motion of the cantilevers beneath was limited by rigid stops, which ensured the exact placement of the working parts.

The vertical load was applied by means of a clamping beam, which also could be rotated in the vertical plane and, on being brought into contact with the head of the loading rod of a given assembly, lowered it.

Penetration assembly. /574 The working part consisted (Fig. 2) of a polished cone 1 with a tip angle $\alpha = 30^{\circ}$. The cone weighed 20 g. The introduction of the cone into the surface of the sample 2 placed in the small bowl 3 was carried out under its own weight. The cone was secured to a membrane 4, which freely lay on a circular support within the head of the assembly 5. A type MFKP strain gage was cemented to the membrane; the strain gage measured the force transmitted from the cone to the membrane. In the initial position the weight of the cone was transmitted to the membrane. During the course of the experiment, the clamping beam mounted on a separate rotating lever was shifted beneath the cone together with the measuring assembly up to the surface of the sample. The zero reading was recorded. With further slow movement, the cone

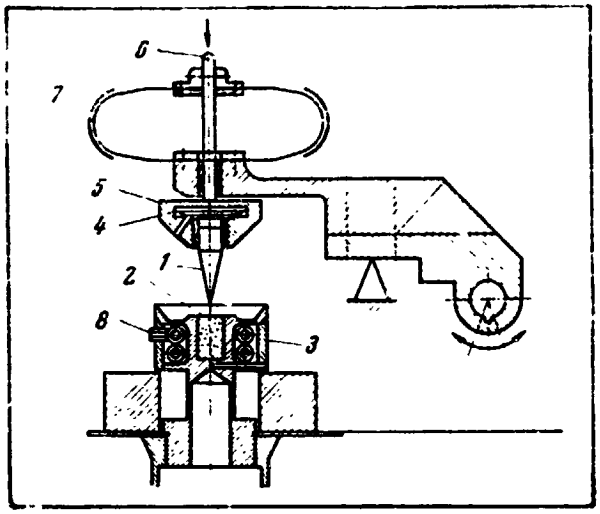

Fig. 2. Assembly for penetration experiments.

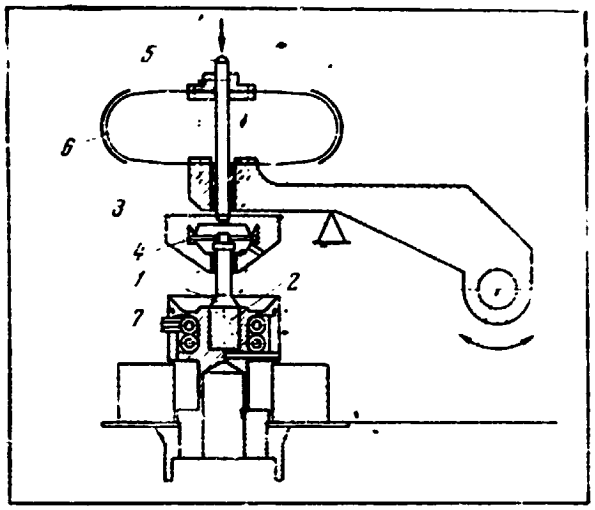

Fig. 3. Assembly for compression tests.

entered into contact with surface material. Gradually the entire weight was transmitted to the surface material, and the measuring membrane was completely ruptured, indicated by the readings of the transducer. The depth to which the cone was immersed was determined by the vertical displacement of rod 6 by means of elliptical spring 7 with type FKP strain gages cemented to it. The maximum depth of immersion was 1.8 cm. The sample in the small bowl could be heated with heater 8.

Compression assembly. The working part (Fig. 3) was a polished piston 1 with a flat base, 11 mm in diameter, applied to the surface of the sample 2. The piston was secured to the membrane 3 with a type MFKP strain gage cemented to it. The membrane was secured on a circular support within the head 4. The vertical displacement of the head was brought about by the action of the clamping beam on the top of the rod 5. Here the membrane was pressed against the piston and compelled it to move into the surface of the sample. The force of indentation was measured with the strain gage membrane, and the piston displacement was measured with elliptical spring 6 bearing type FKP strain gages. The sample could be heated with heater 7. The vertical pressure on the surface material could be varied from 0 to 1.5 kg/cm^2, and the depth of the piston insertion could be varied from 0 to 0.8 cm.

Rotational shearing assembly. The assembly (Fig. 4) was mounted on cantilever 1. Before testing, it was inclined to the working bowl of instrument 2 so that the working part -- ribbed disk 3 -- was brought into contact with the surface of sample 4. The vertical load on the working part was brought about with the

TABLE 4. COEFFICIENT OF RELATIVE COMPRESSIBILITY a_o (in cm^2/kg) IN HELIUM AT NORMAL PRESSURE AND TEMPERATURE +20° C*

Material	Range of normal pressure Δp_i, kg/cm^2			
	0-0.2	0.2-0.4	0.4-0.6	0.6-0.8
Lunar surface material	1.63	0.42	0.24	0.11
Andesite-basaltic volcanic sand	0.82	0.10	0.06	0.04
Crushed basalt	2.10	0.26	0.12	0.08

* The initial condition of the surface material was heaped, friable with the following values of the porosity coefficient: lunar surface material $\epsilon_o = 1.56$; andesite-basaltic sand $\epsilon_o = 1.59$; crushed basalt $\epsilon_o = 2.00$.

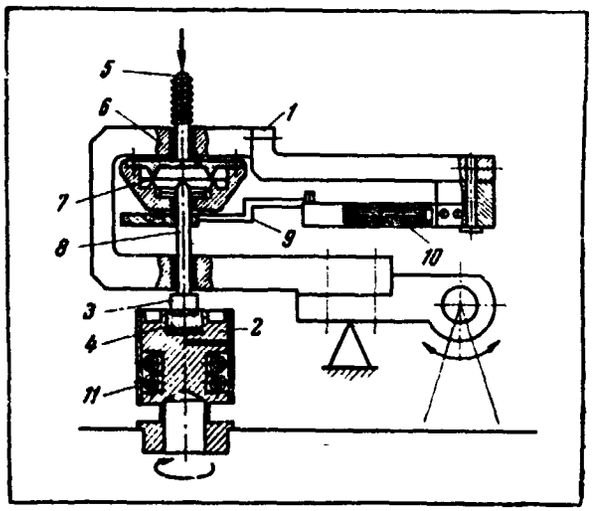

Fig. 4. Assembly for rotational shearing experiments.

clamped beam acting against the loading rod 5. The rod was shifted in the dried bushing 6 and transmitted its pressure via membrane 7 and the second rod 8 onto the ribbed disk.

After application of a specified vertical load, which was measured with the strain gage on membrane 7, the bowl containing the surface material samples was brought into rotational motion about the vertical axis and engaged with the ribbed disk and its rod. Secured to the rod was lever 9 with a support, touching the measuring strain gage beam 10. The FKP strain gages cemented to the beam measured the force of lever pressure. During the experiment, this force rose and, on reaching a maximum, remained constant or decreased. From the vertical force the limiting torque causing shearing of the sample beneath the ribbed disk was calculated. /575

The vertical load on the sample could be varied from 0 to 0.6 kg/cm^2, and the limiting torque -- from 0 to 0.150 kg·cm. The instrument bowl was equipped with heater 11.

The signals from the strain gage transducers for measuring the forces and deformations were fed to amplifier 8 ANCh-7M, and further, to PS-1 recorders. As results of each experiment, two plots of force and deformation as functions of time were obtained; they were interpreted with the aid of previously compiled calibration tables. The precision of the measurement averaged about 10 percent of the limiting values of the quantities.

In all the kinds of tests, the load was applied by successively increasing steps, where each step was maintained until there were no more deformations recorded on the recorder graph. On the average, the duration of the experiment for penetration was 0.5 min, for compression 10 min, and for rotational shearing 3 min. Considering the entire absence of the liquids in the pores of surface material and the impossibility of slowing down the deformations through processes of filtrational consolidation, this duration can be regarded as adequate in order to assume at each stage of the experiment that the deformations had been completed.

Since the lunar surface material was placed in the container in a helium atmosphere and was not brought into contact with the normal atmosphere, all its tests were conducted in helium. In order to find out the effect of vacuum and normal terrestrial atmosphere on mechanical properties, surface material-analogs were tested in all three regimes: in normal atmosphere, helium atmosphere, and in a vacuum of 10^{-5} torr at the temperatures + 20 and + (135-140)° C. The following were conducted: three penetration, two compression, and three experiments on rotational shearing. The above-presented data were obtained from the experiments in which no gross errors were detected.

Test results. Tables of the specific resistance to penetration for all the surface materials investigated were compiled from the penetration tests; then from these tables, a graph was plotted, shown in Fig. 6, indicating the dependence of R on the coefficient of surface material porosity ϵ.

From the compression tests, curves were plotted describing the dependence of the depth of piston immersion on the vertical pressure, shown in Fig. 7 and 8. From the interpretation of these curves, the values of the coefficients of relative compressibility for different pressure intervals, shown in Tables 4 and 5, were obtained. /576

From the tests for rotational shearing, plots were made of the dependence of the limiting resistance to shearing on the normal pressure, examples of which are shown in Fig. 9. Based on these graphs, values were obtained for the angles of internal friction and cohesion, shown in Tables 6 and 7.

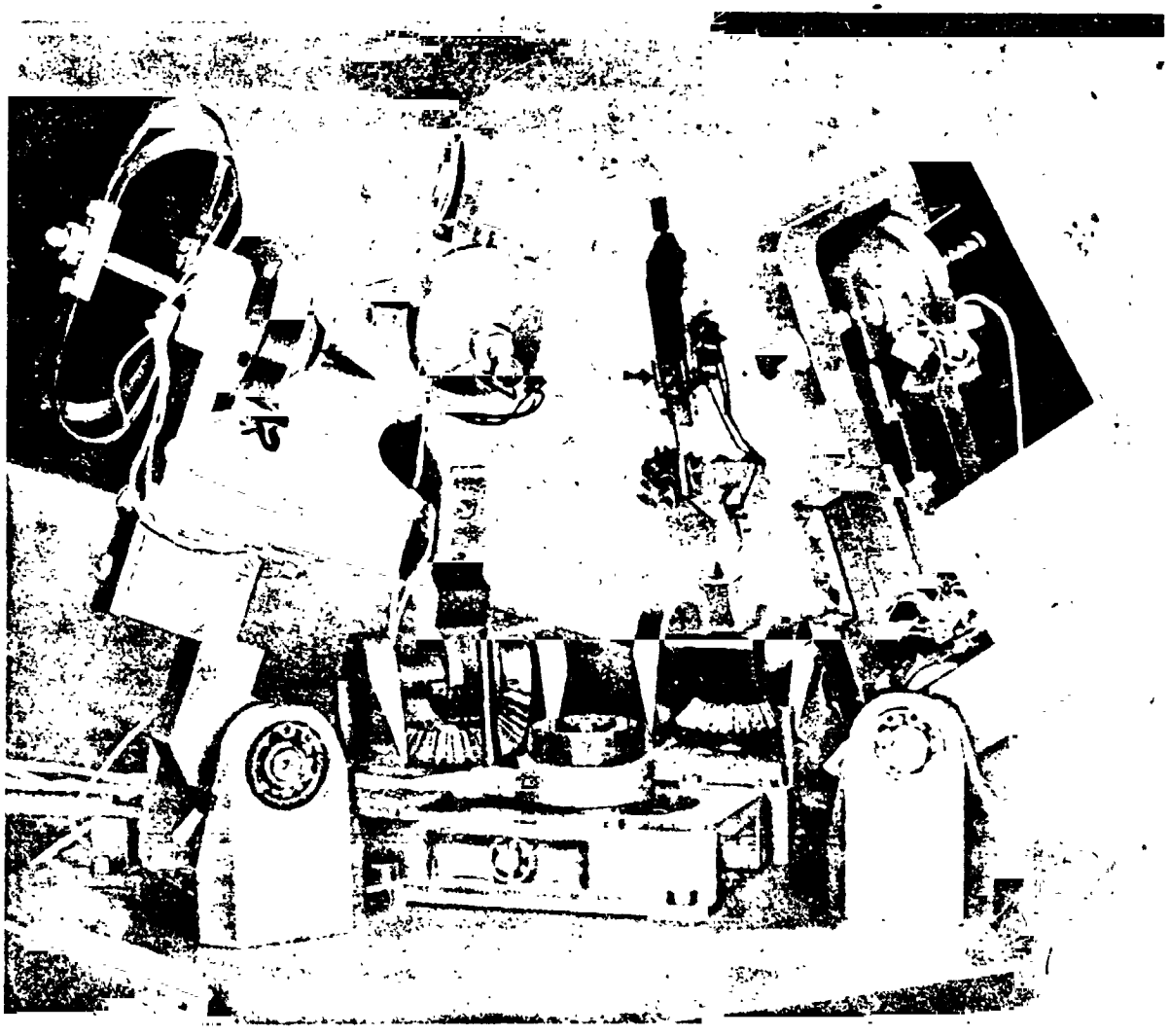

Fig. 5. Internal view of TOR-1 vacuum chamber housing test assemblies.

Penetration tests. The composite plot of the experimental results in helium at the temperatures + 20 and + 140° C and in the vacuum of 10^{-5} torr at + 140° C is in Fig. 6. From the graph it follows that the primary factor determining the specific resistance to penetration for all the materials investigated is their porosity coefficient. For the case of friable heaped surface materials, the specific resistance to penetration decreases to R = 0.012 kg/cm^2, while for surface materials compacted by rapping and area reduction with a stamp, it rose to 0.357-0.383 kg/cm^2. Compared with the effect of porosity, the effect of the

TABLE 5. COEFFICIENT OF RELATIVE COMPRESSIBILITY a_o (in cm^2/kg) IN DIFFERENT ATMOSPHERES AND IN VACUUM FOR SURFACE MATERIAL-ANALOGS*

Material and range of compression stresses, kg/cm^2	Test conditions		
	Helium + 20° C	Helium + 135° C	Vacuum, 10^{-5} torr, + 135° C
Crushed basalt			
0-0.1	2.22	2.55	2.84
0.1-0.2	0.286	0.22	0.47
0.2-1.0	0.064	0.071	0.08
Andesite-basaltic volcanic sand			
0.01	1.17	0.90	0.66
0.1-0.2	0.14	0.21	0.17
0.2-1.0	0.045	0.06	0.06

* The initial condition of the surface materials was friable, heaped with the following values of the porosity coefficient: basalt $\epsilon_o = 2.00$; andesite-basaltic sand $\epsilon_o = 1.39$.

TABLE 6. PARAMETERS OF THE RESISTANCE TO SHEARING IN HELIUM AT NORMAL PRESSURE AND TEMPERATURE + 20° C*

Material	Angle of internal friction, ϕ	Cohesion, c
Lunar surface material	29°30' (35°30')	0.030 (0.010)
Andesite-basaltic volcanic sand	26°00'	0.016
Crushed basalt	29°00'	0

* Before testing, the surface materials were compacted by rapping and by the repeated application of a vertical pressure $\sigma = 0.55$ kg/cm^2. Given in the table are the data for the averaged plots of the function $\tau_{limit} = F(\sigma)$. Given in the parentheses are the values of C and ϕ for the initial section of the plot of the lunar surface material.

medium and the temperature, within the limits tested, proved to be secondary. It can be noted that in the case of soils in the friable heaped state, the resistance to penetration in helium at + 140° C proved to be somewhat higher than at + 20° C, while in vacuum it

was nearly the same as in helium. For the case of compacted soils, the transition from + 20 to + 140° C in most cases led to some reduction in the resistance to penetration, and the same effect was brought about by the transition to vacuum. Overall, all the experimental results involving penetration must be regarded as preliminary, since they were too strongly affected by the conditions of heaping of the soils in the bowl of the instrument and their further processing.

Compression tests. First of all, compression curves were obtained for the lunar surface material and its analogs in a helium atmosphere at normal pressure and temperature + 20° C, shown in Fig. 7. From these curves, the values of a_o given in Table 4 were calculated.

Since no tests of the lunar surface material in vacuum could be made for a number of reasons, special experiments with the analogs in a helium atmosphere at + 20 and + 135° C were carried out, and in the vacuum of 10^{-5} torr at + 135° C to clarify the extent to which the properties of the surface material change in the transition from the helium atmosphere to vacuum. The results of these experiments are given in Fig. 8 and in Table 5.

Analysis of Table 4 shows that the lunar surface material in the friable heaped state has extremely high compressibility, which, however, upon the initial area reduction with a pressure of the order of 0.2 kg/cm^2 is reduced by several times, although even by the end of the experiment, for a compressive stress 0.6-0.8 kg/cm^2, still remains large, considerably exceeding the compressibility of the sandy surface materials common on Earth in the medium-compact and compact states that are customary for the latter. The same is also true of the surface material-analogs -- crushed basalt and volcanic andesite-basaltic sand, whose compressibility characteristics are close to the characteristics of lunar surface material and indicate high compressibility of these /577
materials in the friable heaped state. The test results indicate that in the conditions given above, these materials as analogs of the lunar surface material were successfully chosen and can serve as its substitutes in compressibility experiments.

Based on analysis of Table 5, it can be noted that in the case of both materials, in all test conditions for the same intervals of loading, the coefficients of compressibility have the same order of magnitude. In first importance is the initial area reduction, and the coefficient of relative compressibility takes on maximum values, while it then is sharply reduced, and in the last stage reaches the value 0.045-0.080 cm^2/kg. However, even these latter figures still considerably exceed the values $a_o \simeq 0.01$ cm^2/kg that are customary for mean-density terrestrial silty sands.

The effect of heating and vacuum on the properties of the samples shows up in different ways. In the case of crushed basalt, compressibility rises somewhat overall loading intervals, which probably can be associated with some unconsolidation of the samples on heating and evacuation. In the case of andesite-basaltic volcanic sand, at the first stage of loading compressibility becomes less, while in successive stages it increases somewhat. However, in both cases no abrupt change in the properties is noted, and in general it can be assumed that tests in helium atmosphere at normal pressure and temperature + 20° C yield approximately the same results as tests in the vacuum of 10^{-5} torr at + 135° C. The reason for this must be sought for, on the one hand, in the insufficiently high vacuum, and on the other hand, in the fact that within the sample of the finely dispersed surface material beneath the instrument piston, in all probability the vacuum is poorer than in the TOR-1 chamber overall. /578

Supplementing the tests described above, control experiments were made in which the surface material-analogs were compressed in the TOR-1 unit in an air atmosphere at + 20° C and 75 percent humidity. They showed that in most cases the compressibility of both analogs in air is appreciably higher than in helium and in vacuum, which is accounted for by the effect of the hygroscopic moisture. It was noted that both analogs, when dried to constant weight, intensively absorbed moisture from air and the hygroscopic moisture content in the different experiments varied from 1.5 to 3.0 percent.

It should be noted that carrying out compression in the miniaturized instrument must lead to understating of the compressibility coefficients owing to the friction of the surface material against the wall of the working cylinder. Preliminary data from the determination of the scaling factor indicate that in our case we can expect understating of the compressibility, where the scaling factor probably shows up differently at different stages of the experiment. Tables 4 and 5 give the values of a_o without allowing for the effect of the scaling factor.

Experiments on rotational shearing. The first tests were conducted to determine the properties of the lunar surface material and its analogs in the helium atmosphere at normal temperature and temperature + 20° C (see Fig. 9).

Analysis of Table 6 shows that on the average, the lunar surface material and its analogs have closely similar values of the resistance to shearing and that they are all characterized in the given test conditions by low cohesion from 0 to 0.016 kg/cm^2. Somewhat unexpected were the values of the angles of internal

TABLE 7. PARAMETERS OF RESISTANCE TO SHEARING IN DIFFERENT TEST CONDITIONS

Material	Test conditions					
	Air, 20° C		Vacuum, 10^{-5} torr, 20° C		Vacuum, 10^{-5} torr, 140° C	
	ϕ	c	ϕ	c	ϕ	c
Andesite-basaltic volcanic sand	27°30'	0	25°30'	0.004	23°40'	0.004
Crushed basalt	30°30'	0	26°50'	0.036	27°00'	0.004

friction, which averaged 26-30°. The data on lunar surface materials and the investigation of their terrestrial analogs earlier given in the literature generally fall in the area of 35-37° and even higher. Accordingly, additional experiments with analogs involving rotational shearing in an air atmosphere at + 20° C and in a vacuum of 10^{-5} torr at + 20 and + 140° C were carried out.

Table 6 gives the data for the averaged plots of the function τ_{limit}). As we can see from Table 7, the transition from the tests in the air atmosphere to the tests in vacuum led to the appearance of low cohesion and a reduction in the angle of internal friction. It should, however, be borne in mind that the graphs were plotted based on three points each and that their averaging by the inclined lines led to a distortion of the initial sections. In practice, the resistance to shearing under all three test regimes differed little. From these experiments, as can be seen /579 from the figures presented, low values of the angle of internal friction also resulted. The following factors can serve as the reasons for this:

1) the experiments were conducted with finely dispersed silty surface materials, while the earlier experiments involved coarser sandy varieties, which always have higher angles of friction;

2) the surface materials tested were compacted with a low pressure of 0.55 kg/cm^2 and had sufficiently high porosity, while it is known that with increase in porosity the angle of internal friction of granular surface materials becomes less; and

3) the miniature dimensions of the sample can lead to the appearance of a scaling factor that affects the experimental results.

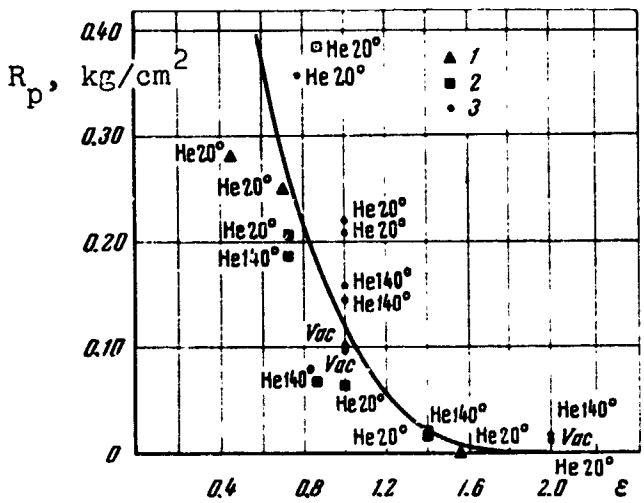

Fig. 6. Dependence of specific resistance to penetration R on the porosity coefficient of surface material ε and the experimental conditions
1. Lunar surface material
2. Andesite-basaltic volcanic sand
3. Crushed basalt. He 20° -- -- helium at normal pressure and temperature +20°; He 140° -- as above at +140°, Vac -- vacuum at +140° C.

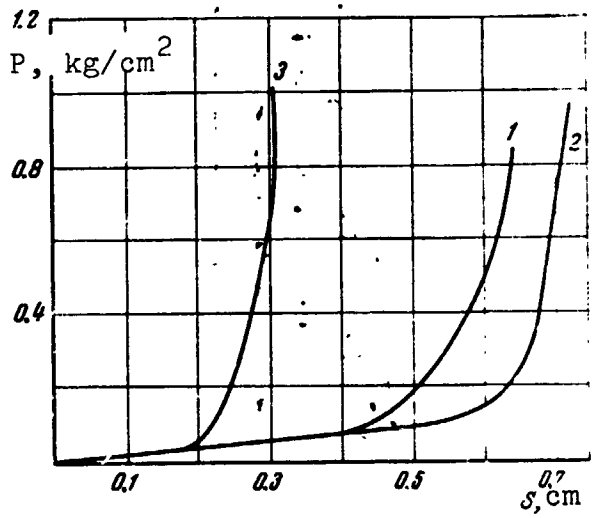

Fig. 7. Dependence of vertical compression of sample S on mean pressure beneath piston in compression testing P in helium atmosphere at normal pressure and temperature of 20° C.
1. Lunar surface material
2. Andesite-basaltic volcanic sand
3. Crushed basalt

Effect of scaling factor. With decrease in the dimensions of the test instruments and with increase in the ratio of the sample height to its diameter, the effect of the walls of the working cylinder in which the experiments are conducted on penetration, compression, and shearing becomes greater. The friction of the surface material against the walls leads to its more friable placement when freely heaped into the instrument; it causes additional resistance to compression in the compression test and can be reflected in the results of the rotational shearing experiment, since the movement of the peripheral grains of the sample material is restricted. In the penetration experiments, the walls interfere with the free expansion of the surface material laterally and increase the resistance of the surface material to the insertion of a cone.

Evidently, the use of instruments of these small dimensions for investigating the mechanical properties of surface material, such as were compelled in experiments involving the TOR-1, is

encountered for the first time in soil mechanics. Until now, the smallest diameter of a sample was assumed to be approximately 40 mm, which is 3.5 times greater than in the TOR-1. Accordingly, experimental investigations were conducted dealing with the scaling factor, which are still continuing. It was established for the penetration experiments that the ratio of the specific resistance to penetration when a 40 mm diameter bowl is used to the same value for an 11.3 mm diameter bowl is 0.33-0.45 for a cone with a 30° angle, weighing 20.5 g. Appropriate corrections were made into the results of the experiment and taken into account in plotting of the graph in Fig. 6.

As for the coefficient of relative compressibility, we can anticipate the opposite effect of sample scale, but the final values of the correction coefficients have not yet been established, and the data obtained without corrections are listed in Tables 4 and 5. The same is true of the rotational shearing experiments.

Conclusions. 1) The sample of Sea of Fertility lunar surface material that was investigated is characterized by a specific weight in the friable heaped state $\gamma_{friable} = 1.26$ g/cm^3 and in the compact state $\gamma_{compact} = 1.90$ g/cm^3, to which correspond the porosity coefficients, respectively, $\epsilon_{friable} = 1.46$ and $\epsilon_{compact} = 0.63$. Its terrestrial analogs -- andesite-basaltic volcanic sand and crushed basalt -- have lower values of specific weight in both the friable and the compacted states (see Table 3). /581

2. The specific resistance to penetration of lunar surface material is determined mainly by its density. In the friable heaped state, the surface material exerts virtually no resistance to the penetration of a cone, while in the compacted state R = 0.25-0.28 kg/cm^2. The surface material-analogs have similar values of specific resistance to penetration in identical test conditions.

3. The coefficient of relative compressibility of lunar surface material is very high at the first loading stage and in the interval of normal pressure 0-0.2 kg/cm^2 it is 1.63 cm^2/kg. Then the surface material becomes compacted and the coefficient of relative compressibility is reduced by severalfold. But even at a pressure of 1 kg/cm^2 it is 0.11 cm^2/kg, which is one order higher than the coefficient of compressibility for common sand in terrestrial conditions. The surface material-analogs have the same properties and closely simulate the lunar surface material with respect to compressibility at all loading stages.

4. The lunar surface material has an angle of internal friction of 35° at the first stage of the experiment, and 29° on the average for a cohesion of 0.01 and 0.03 kg/cm^2, respectively. The surface

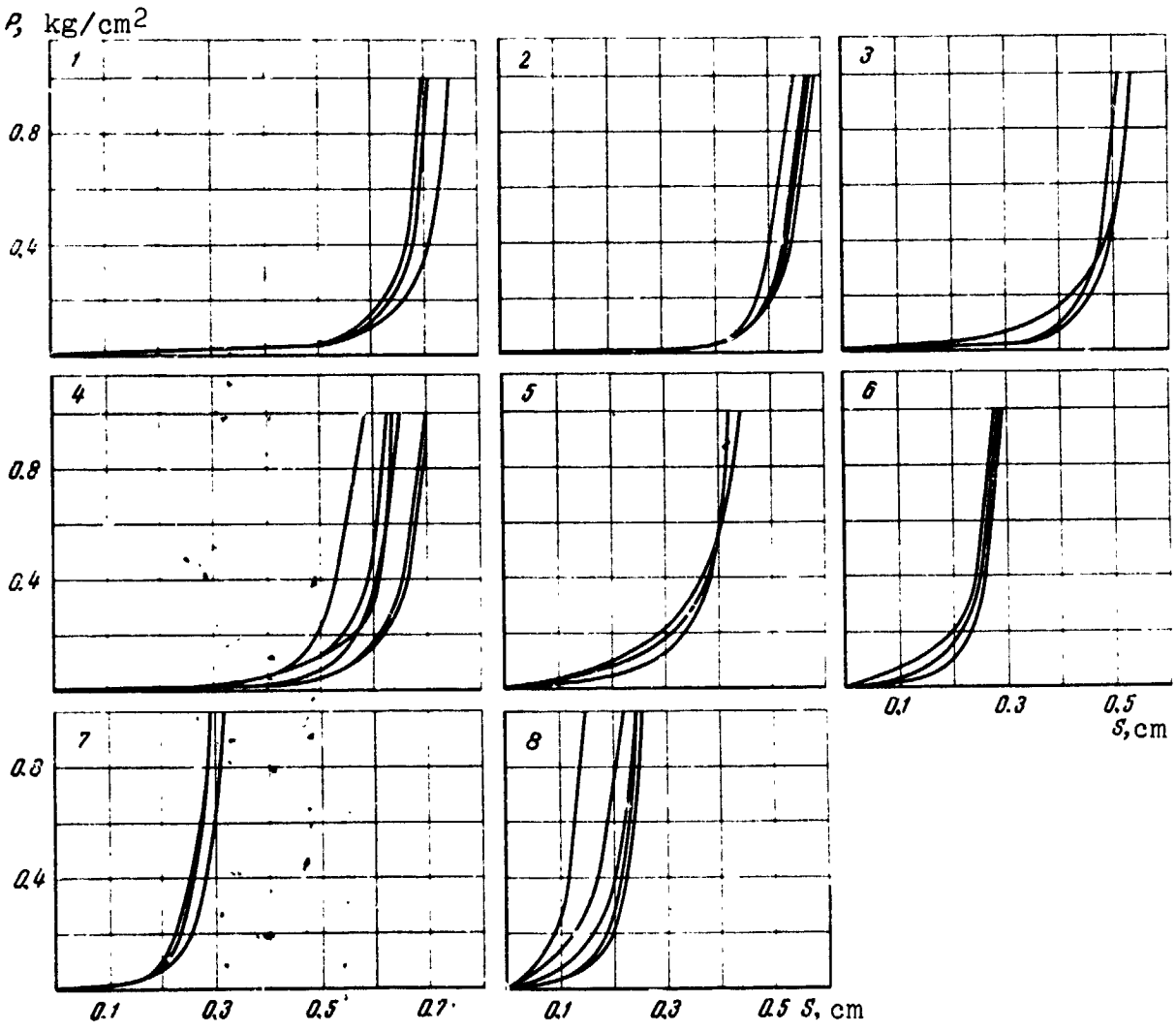

Fig. 8. Dependence of vertical compression of sample S on mean pressure beneath piston in compression testing P for different experimental conditions.

1. Crushed basalt in air at normal atmospheric pressure and temperature + 20° C;
2. As above in helium at atmospheric pressure and + 20° C;
3. As above in helium at atmospheric pressure and + 135° C;
4. As above in a vacuum of $2 \cdot 10^{-5}$ torr at + 135° C;
5. Andesite-basaltic volcanic sand in air at normal atmospheric pressure and temperature + 20° C;
6. As above in helium at atmospheric pressure and + 20° C;
7. As above in helium at atmospheric pressure and + 135° C;
8. As above in a vacuum of $2 \cdot 10^{-5}$ torr at + 135° C.

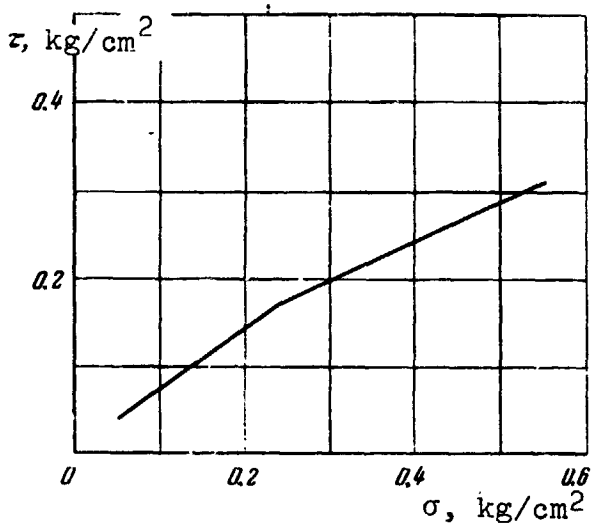

Fig. 9. Example of plot of the dependence of limiting resistance to shearing τ_{limit} on normal pressure σ for lunar surface material in helium atmosphere at + 20° C.

material-analogs have somewhat smaller values for both parameters. It should be noted that these data are somewhat smaller than those ordinarily published for lunar surface materials.

5. The miniature dimensions of the instrument dictated by the small volume of the surface material may have been reflected in the results of the determination of the mechanical parameters R, a_0, c, and ϕ. The effect of the scaling factor for penetration was found also in interpreting the experimental results; for compression and shearing, work on the determination of the correction factors for a_0, ϕ, and c is continuing.

6. Overall, the results of tests in helium at +20° C differ insubstantially from the test results for helium at +140° C and in a 10^{-5} torr vacuum at +140° C. In all probability, this is due to the impossibility of achieving a vacuum in the bulk of the surface material sample enclosed in a tight collar. It is necessary to continue experiments testing surface materials in vacuum by other techniques that would ensure total degassing of samples and the carrying out of these experiments in a higher vacuum.

7. At the present level of test apparatus, mass testing of lunar surface materials and their analogs is usefully conducted in a helium atmosphere at +20° C, ensuring identical conditions and elimination of random errors; also expedient are individual experiments aimed at finding the effect of high vacuum on the properties of lunar surface materials, carried out in accordance with paragraph 6.

REFERENCES

1. Vinogradov, A. P., "Preliminary Data on Lunar Surface Material Returned by Luna 16 Automatic Station," Geokhimiya (3), (1971).

2. Stakheyev, Yu. I., Vul'fson, Ye. K., Ivanov, A. V., and Florenskiy, K. P., "Granulometric Characteristics of Lunar Surface Material from the Sea of Fertility," present collection, p. 44.

3. Zelenin, A. N., Karasev, G. N., and Krasil'nikov, L. V., Laboratornyy praktikum po rezaniyu gruntov /Laboratory Handbook on Cutting Surface Materials/, "Vysshaya shkola" Press, 1969.

4. Drozhzhina, M. P., Dymov, V. V., Krylov, V. M., Markachev, V. V., Silin, A. A., and Shvarev, V. V., "TOR- Instrument for Investigating the Engineering-Physical Properties of Lunar Surface Material," Dokl. AN SSSR 199(5), (1971).

5. Druzhininskaya, V. A., Markachev, V. V., Serenov, A. V., Surkov, Yu. A., and Cherkasov, I. I., "Preliminary Results of Investigating the Mechanical Properties of Lunar Regolith," Dokl. AN SSSR 199(6), (1971).

All-Union Scientific Research Institute of Physical-Optical Measurements, Moscow

Moscow Institute of Transportation Engineers, Moscow